ACS Chemical Neuroscience

Research Article

pubs.acs.org/chemneuro

Ellagic Acid Mitigates SNO-PDI Induced Aggregation of Parkinsonian Biomarkers

Parijat Kabiraj,[†] Jose Eduardo Marin,[‡] Armando Varela-Ramirez,[‡,§] Emmanuel Zubia,[†] and Mahesh Narayan*,[†]

[†]Department of Chemistry, [‡]Department of Biological Sciences, [§]Cytometry, Screening and Imaging Core Facility and Border Biomedical Research Center, The University of Texas at El Paso, El Paso, Texas 79968, United States

Supporting Information

ABSTRACT: Nitrosative stress mediated S-nitrosylation (SNO) of protein disulfide isomerase (PDI), a housekeeping oxidoreductase, has been implicated in the pathogenesis of sporadic Parkinson's (PD) and Alzheimer's (AD) diseases. Previous cell line studies have indicated that SNO-PDI formation provokes synphilin-1 aggregation, the minor Parkinsonian biomarker protein. Yet no work exists investigating whether SNO-PDI induces α-synuclein aggregation, the major Lewy body constituent associated with Parkinson's pathogenesis. Here, we report that SNO-PDI formation is linked to the aggregation of α-synuclein and also provokes α-synuclein:synphilin-1 deposits (Lewy-body-like debris) normally found in the PD brain. Furthermore, we have examined the ability of a small molecule, 2,3,7,8-tetrahydroxy-chromeno[5,4,3-cde]chromene-5,10-dione (ellagic acid; EA) to scavenge NOx radicals and to protect cells from SNO-PDI formation via rotenone insult both, cell-based and cell-independent in vitro experiments. Furthermore, EA not only mitigates nitrosative-stress-induced aggregation of synphilin-1 but also α-synuclein and α-synuclein:synphilin-1 composites (Lewy-like neurites) in PC12 cells. Mechanistic analyses of the neuroprotective phenomena revealed that EA lowered rotenone-instigated reactive oxygen species (ROS) and reactive nitrogen species (RNS) in PC12 cells, imparted antiapoptotic tributes, and directly interfered with SNO-PDI formation. Lastly, we demonstrate that EA can bind human serum albumin (HSA). These results collectively indicate that small molecules can provide a therapeutic foothold for overcoming Parkinson's through a prophylactic approach.

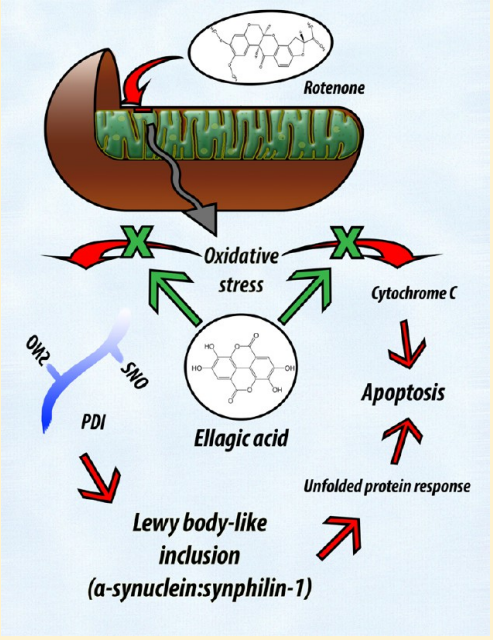

KEYWORDS: *Parkinson's disease, synphilin-1, α-synuclein, ellagic acid, protein disulfide isomerase, rotenone, S-nitrosylation, apoptosis, ER stress, human serum albumin*

With no cure in sight and care burdens constantly rising and currently estimated at $23 and $216 billion, respectively, Parkinson's and Alzheimer's diseases are emerging as a leading cause of morbidity and mortality in the United States.[1,2] Furthermore, recent studies revealed that Hispanics and other minorities are especially prone to neuropathies due to a variety of geo-socioeconomic factors including exposure to pesticides in farms and fields and associated reactive oxygen species (ROS) and reactive nitrogen species (RNS) insult.[3,4]

The housekeeping chaperone protein disulfide isomerase (PDI) is normally responsible for maturation of proteins and thus regulates traffic flow in the cell.[5,6] However, in post-mortem brains of Parkinson's and Alzheimer's disease victims, PDI has been found to undergo S-nitrosylation (SNO) of its catalytic cysteines in response to nitrosative stress.[7−11]

In follow-up cell line studies, the chemical modification of PDI promoted the aggregation and accumulation of the minor, but signature, Parkinsonian-specific biomarker synphilin-1 in a nitric oxide (NO)-sensitive manner.[9−11] However, overexpression of wild-type PDI (non-SNO-PDI) attenuated the accumulation of synphilin-1-containing aggregates in the SHSY-5Y cell line.[10]

In contrast to these studies involving synphilin-1, a gap exists in studies examining the aggregation of other neurodegeneration-specific biomarkers in response to SNO-PDI formation.[12,13] Specifically, no studies have examined the impact of SNO-PDI formation on the aggregation of α-synuclein, the major Parkinsonian biomarker and principal Lewy body constituent.[14−17] Here, we examined whether SNO-PDI formation provokes α-synuclein aggregation and Lewy-like

Received: April 11, 2014
Revised: September 17, 2014
Published: September 23, 2014

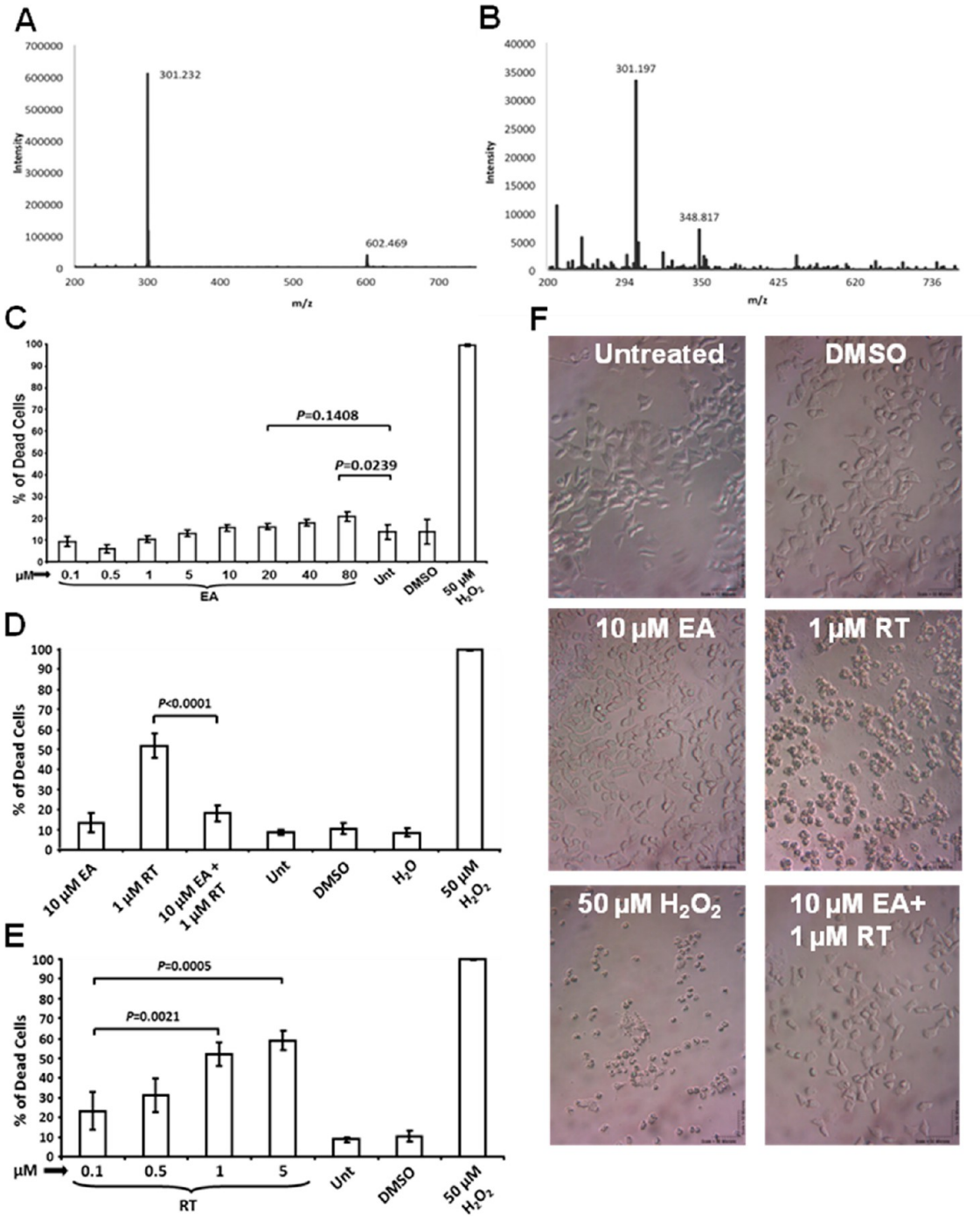

Figure 1. Ellagic acid (EA) scavenging NO radical in vitro (A, B). Cytotoxicity and protective ability of ellagic acid on PC12 cell line against rotenone insult (C–F). The cytotoxicity and preventive effect of EA was testified on the PC12 cell line, measured by using differential nuclear staining (DNS) assay adapted to high throughput screening (HTS). Cytotoxicity of EA at different concentration after 24 h of treatment (C). Statistical significance compared with untreated are illustrated as *P*-value. Cytotoxicity of rotenone (RT) at different concentration after 24 h of treatment (D). Preventive effect of EA against RT toxicity in PC12 cells (E). Bright field images of PC12 cells taken by using compound microscope after different treatments, as indicated below each image (F). White scale bar in each image indicate 50 μm distances. Data were analyzed by using BD AttoVision v1.6.2 software. Each experimental point was assessed in quintuplicate.

neurite formation and, thus, causes the nitrosative stress-associated Parkinson's pathogenesis.

Also noteworthy is the prominent gap in efforts designed to prevent nitrosative damage to PDI. This is despite the fact that over 7 years have passed since the discovery of the proven association of this chemical mutation with synphilin-1 aggregation.[10] Lately, the housekeeping chaperone PDI has emerged as a critical neuroprotectant whose catalytic integrity is pivotal to neuronal function.[18−21] Our objective was to test compounds that can prevent SNO-PDI formation and can thus mitigate the accumulation of misfolded protein debris such as Parkinsonian synphilin-1 and perhaps α-synuclein. Importantly, this research may fill the void in molecular-level efforts toward preventing PD, the Lewy body variant of Alzheimer's disease

(LBVAD), and other neurodegenerative disorders given that a number of other studies have confirmed that the functional security of cellular housekeeping machinery is pivotal to neuronal health.[21−23]

Ellagic acid (EA), 2,3,7,8-tetrahydroxy-chromeno ($C_{14}H_6O_8$), a plant polyphenol present in fruits such as pomegranates, strawberries, raspberries, blackberries, and so forth exerts strong antioxidative, anticarcinogenic, and antifibrosis properties.[24,25] Growing interest in natural products as effective prophylactic in many fields instigated our work on EA as a potential candidate for this study. In addition, we investigated the ability of EA to bind HSA with the objective of improving its systemic distribution. HSA is a prominent carrier protein in the circulatory system;[26,27] thus, having the ability to strongly interact with HSA plays an important role in the transport and delivery of molecules such as EA.

Our results indicate that a rotenone-insult induced increase in ROS and RNS levels in the cell is associated with SNO-PDI formation as well as that SNO-PDI formation triggers the accumulation of the major PD biomarker α-synuclein. Our data also reveal that SNO-PDI formation provokes colocalization and the concomitant formation of α-synuclein:synphilin-1-containing Lewy-body-like aggregates, suggesting that SNO-PDI formation is a key milestone in the pathogenesis of nitrosative stress-induced PD. In addition, we demonstrate that EA intervenes in nitrosative stress-associated endoplasmic reticulum (ER) stress, accumulation of ubiquitinated proteins, apoptosis, and the formation of Lewy-like aggregates. Furthermore, administration of ellagic acid to the cell line prior to rotenone insult mitigated SNO-PDI formation and the formation of synphilin-1, α-synuclein, and α-synuclein:synphilin-1-containing Lewy-body-like aggregates. Finally, the demonstrated ability of EA to reversibly bind HSA makes it a viable choice to use as a prophylactic in ROS/RNS-induced neuropathies.

RESULTS AND DISCUSSION

Nitrosative stress-induced chemical mutation of a key housekeeping chaperone, PDI, has been convincingly implicated in the pathogenesis of sporadic Parkinson's and Alzheimer's diseases.[7−11] While SNO-PDI formation triggers the aggregation of the minor Parkinsonian biomarker synphilin-1,[10] heretofore it remained unknown whether S-nitrosylation-induced loss of catalytic function of PDI provoked the accumulation of the key Parkinsonian protein α-synuclein. Using a variety of biochemical and analytical techniques, we investigated the relationship between SNO-PDI formation and the aggregation of α-synuclein and α-synuclein:synphilin-1 containing (Lewy-body-like) composites. Furthermore, while previous studies have demonstrated that overexpression of wild-type PDI attenuates the accumulation of synphilin-1,[10] it remains an unfeasible mechanism for therapeutic intervention. In contrast, small molecules such as EA may provide therapeutically desirable alternatives for prevention of neurodegeneration. We have assessed the ability of the small molecule polyphenolic phytochemical ellagic acid to protect PDI from becoming S-nitrosylated. We have also analyzed its efficacy in mitigating SNO-PDI associated aggregation of synphilin-1, α-synuclein, and synphilin-1:α-synuclein composites (Lewy-body-like neurites) and its ability to bind to a carrier protein.

Cytotoxicity of EA and Its Free Radical Scavenging Potential. Ability of EA as a potential free radical scavenger was determined by mass spectrometric analysis, carried out in a controlled environment (Figure 1A, B). A molecular weight of 301.232 Da in the negative ion mode suggests double deprotonation of EA.[28] In addition, a peak at 602.469 Da was observed which suggests the presence of EA dimers. Nitric oxide reacts with cellular superoxide (O_2^-) to form the peroxynitrite ($ONOO^-$) resulting in ring nitration.[29] We have employed tetranitromethane (TNM), a model mimic of peroxynitrite, as a NOx donor to examine the ability of EA to scavenge RNS.[30−32] Upon exposure of EA to TNM, a mass increase of ∼47 Da was observed which indicates the presence of a NO_2 adduct and two protons on EA. The data indicates that, by becoming nitrated in the presence of a NOx radical donor, EA can indirectly impact nitric oxide levels. This is because, even though EA does not react with NO directly, it (partially) consumes total available NO by scavenging the reaction product between NO and superoxide, that is, peroxynitrite, as evidenced by the reaction product between EA and model peroxynitrite mimic, TNM.[30−32]

Cytotoxicity of EA and its protective effect against rotenone (RT) in PC12 cells was determined using a high-throughput screening assay. Cells exposed to increasing concentrations of 0.1−80 μM EA exhibited a concomitant progressive cytotoxicity from 9% to 24% (Figure 1C). However, up to 20 μM, there is no difference compared to untreated and vehicle controls (as evaluated by the *P*-value). Statistical significance of 80 μM EA treatment against untreated (Unt) condition is also very low. In contrast, the addition of 5 μM RT induced 60% cell death in the PC12 cell line after 24 h incubation (Figure 1D). The administration of 10 μM EA prior to 1 μM RT exposure resulted in ∼20% cell death whereas administration of 1 μM RT resulted in ∼55% cell death (Figure 1E). These data imply that EA pretreatment was able to rescue cell death by ∼35% ($P < 0.0001$). Supporting Information Figure 1 is a representative image of untreated and 50 μM H_2O_2 (positive control) treated cells. *P*-value was calculated to determine statistical significance of the results between two experimental sample groups. Morphology of cells upon administration of EA prior to RT insult is further evidence of the protective aspects of EA against RT-induced cell death (Figure 1F). The bright field compound microscopy picture provides evidence of cellular morphology when cells were exposed to different conditions. The pretreatment with 10 μM EA for 6 h enabled the PC12 cells to retain their morphology (as untreated PC12) even after 1 μM RT insult. Cells exposed to 1 μM RT for 24 h showed morphology similar to that observed in the positive control. Hydrogen peroxide (H_2O_2) was used as a positive control for this experiment at a concentration of 50 μM (Figure 1F). All the data collectively indicate that ellagic acid preincubation is able to protect PC12 cells against rotenone insult (Figure 1).

Cell-Based Reactive Oxygen and Nitrogen Species Scavenging Assays. The effect of EA on the total cellular ROS production was measured using 2′,7′-dichlorodihydrofluorescein diacetate (DCFH-DA) fluorescence assay. The cell-permeable DCFH-DA reagent is reduced by cellular esterase to 2′,7′-dichlorofluorescein (DCF) and is trapped within the intracellular space. Additionally, several ROS agents such as hydrogen peroxide, superoxide anion (O_2^-), hydroxyl radical ($^{\bullet}OH$), as well as other peroxides can also oxidize DCF, resulting in the origin of the highly fluorescent DCF product.[33,34] Hence, an increment in cellular fluorescence intensity reflects proportional to a ROS increment. Relative

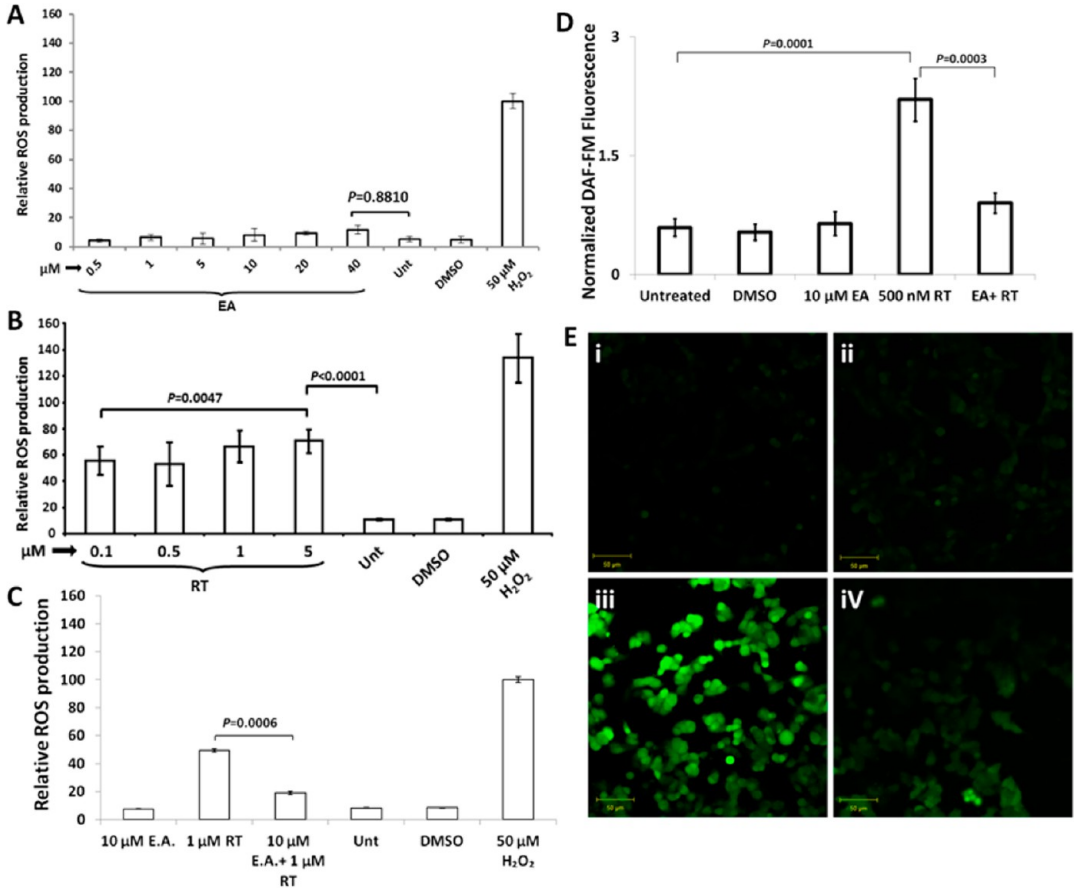

Figure 2. EA treatment attenuates reactive oxygen species (ROS) and reactive nitrogen species (RNS) production in PC12 cells. ROS levels were measured by DCFH-DA staining assay and analyzed at 24 h after EA treatment (A). Levels of ROS in EA treated cells are presented as fold change compared to the levels in positive control cells. Levels of ROS in RT treated cells are presented as fold change compared to the levels in positive control cells (B). The ROS quenching activity of EA pretreated PC12 cells followed by 24 h of RT exposure are presented as fold change compared to the levels in positive control cells (C). RT increases RNS production, which is attenuated by EA pretreatment (D). Representative confocal images confirmed the intracellular RNS production on different treatment (i, DMSO; ii, 10 μM EA; iii, 500 nM RT; iv, EA+RT; E). Statistical significance compared with untreated is illustrated as *P*-value. Each bar represents the average of five replicas, and the error bars their standard deviation.

levels of intracellular ROS increased marginally at and above 20 μM EA administration relative to the vehicle (~4%) and untreated controls (~6%; Figure 2A). *P*-value is not significant up to 40 μM EA treatment when compared with untreated control. The corresponding levels of relative ROS production were ~60−80% as a function of RT (Figure 2B). Preadministration of 10 μM EA to the cell line was able to diminish relative ROS levels significantly from ~50% at 1 μM RT alone to ~20% (EA pretreatment + RT; Figure 2C). The EA dependent diminution in ROS was highly significant in comparison with 1 μM RT treatment (P = 0.0006). The membrane-permeable 4-amino-5-methylamino-2″,7″-difluorofluorescein (DAF-FM) diacetate is transformed by cellular esterases to the fluorescent dye DAF-FM and becomes a direct indicator of intracellular nitric oxide (NO) production.[35] Our data showed significant increase of DAF-FM fluorescence after 500 nM RT treatment in PC12 cells (P = 0.0001; Figure 2D). In contrast, pretreatment with EA dramatically lowers fluorescence levels, indicating its RNS scavenging ability (P = 0.0003). Representative confocal microscopy images confirmed the fluorescence intensity of DAF-FM in PC12 cells upon different treatments where panels (i)−(iv) stand for dimethyl sulfoxide (DMSO), 10 μM EA, 500 nM RT, and 10 μM EA treatment prior to 500 nM RT exposure, respectively (Figure 2E).

Previous work has demonstrated that RT insult primarily results in mitochondrial stress leading to efflux of NOx-based radicals;[3,36] thus, the results observed in the cell-dependent in vitro analyses are consistent with the cell-independent in vitro analysis using the NOx donor model. Our findings suggest that EA is able to mitigate elevated intracellular levels of ROS and RNS (Figure 2). Note that the exact mechanism, nevertheless, is not delineated through cellular studies. It is conceivable that NO levels, which constitute a part of the total RNS, may be reduced in the presence of EA, albeit indirectly, through ring nitration of ellagic acid by peroxynitrite (a product of nitric oxide and superoxide).

Inhibition of Apoptosis and Endoplasmic Reticulum (ER) Stress through EA Intervention. The pathway by which rotenone insult leads to cell death was investigated (Figure 3). The addition of rotenone (500 nM) resulted in early stage apoptosis (Figure 3A, B). However, prior treatment of cells with 10 μM EA resulted in a notably rescue of cells from a rotenone-induced apoptotic cell death. High statistical significance was found when the RT and EA pretreatment + RT treatment conditions were compared (P = 0.0011). Cells

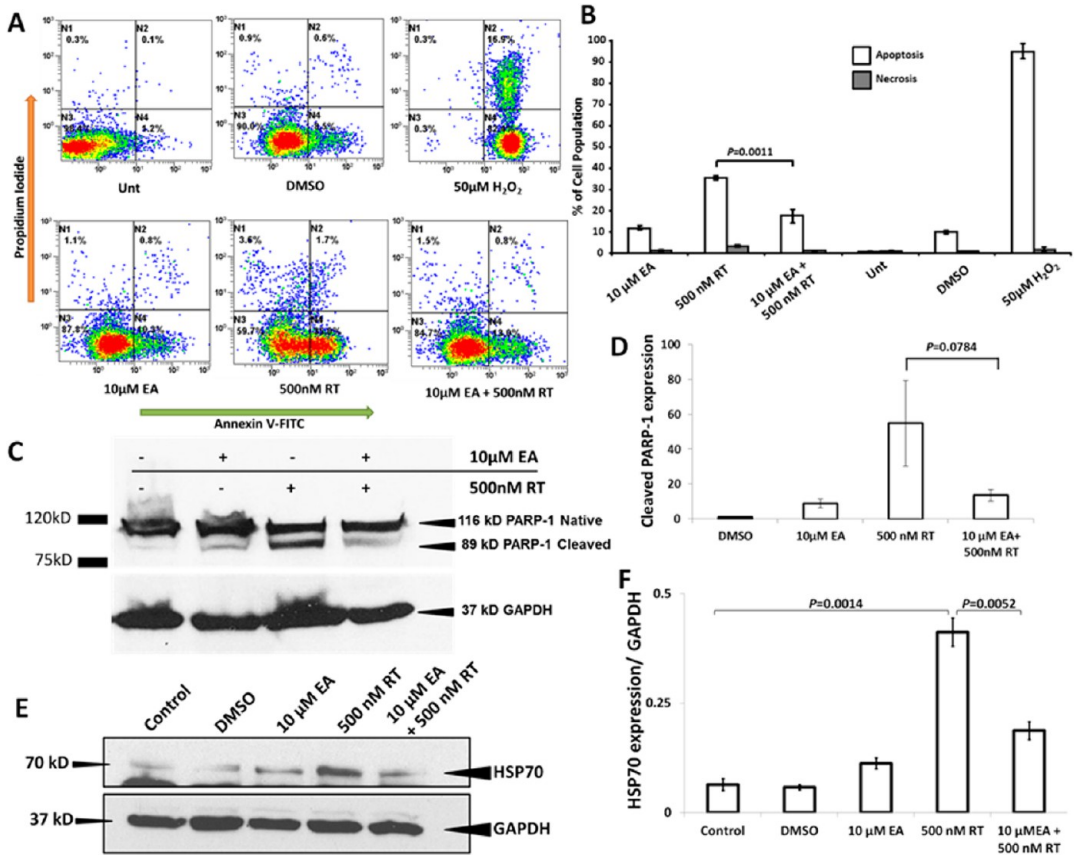

Figure 3. Antiapoptotic ability of EA through maintaining endoplasmic reticulum (ER) homeostasis. Representative flow cytometric histograms used to measure apoptosis/necrosis distribution: untreated control, vehicle control (DMSO), positive control (50 μM H_2O_2), EA, rotenone, and pretreatment with EA and then 24 h rotenone exposure (A). Quantification of apoptotic−necrotic assay under previously mentioned conditions (B). Protective effect of EA (10 μM) against rotenone (500 nM) induced poly(ADP-ribose) polymerase (PARP) cleavage, hallmark of apoptosis progression, in PC12 cells (C). PARP-1 cleavage bands were densitometrically analyzed via Western blot analysis using ImageJ software (D). Rotenone (RT) induced overexpression of heat shock protein 70 (HSP70), an ER resident protein, is mitigated by 10 μM EA pretreatment (E). Expression of ER stress marker protein, HSP70, is quantified under different treatment using ImageJ (F). Statistical significance between samples is illustrated as *P*-value (n = 3).

treated with DMSO (0.1% v/v), 10 μM EA and untreated cells did not show substantial increase either in necrosis or apoptosis. H_2O_2 at a concentration of 50 μM was used as a positive control where substantial increase in early and late apoptosis was denoted in the lower right and top right quadrants of the matrix plot.

Considering that cleavage of poly(ADP-ribose) polymerase (PARP) is a hallmark for apoptotic pathway activation,[37,38] we examined the ability of EA to prevent RT induced apoptosis by measuring cleavage of native PARP-1 (Figure 3C, D). Cleavage of PARP, and therefore activation of apoptosis, occurred when cells were treated with 500 nM RT. This apoptotic biochemical marker was evidenced by a dense band of the cleaved PARP-1 at 89 kDa (Figure 3C; third lane from left). In a control, the addition of 10 μM EA induced ∼15% cleavage of PARP-1 relative to DMSO treatment (Figure 3D). Densitometric analysis of the protein bands revealed that pretreatment with EA for 6 h clearly protected PC12 cells from RT insult. About a 35% reduction in PARP-1 cleavage was observed when compared to RT insult alone. These results support the flow cytometric analysis performed to analyze the ability of ellagic acid to protect PC12 cells against apoptosis and necrosis under RT insult.

As a part of their defense mechanism, cells often activate an apoptotic pathway when they fail to circumvent ER stress. The role of RT as an ER stressor has been documented in previous studies.[39] To evaluate the role of EA in preventing RT mediated ER stress, we checked the expression of HSP70 in PC12 cells (Figure 3E, F). Overexpression of heat shock protein 70 (HSP70) is an indication of ER stress.[39] Treatment with 500 nM RT for 24 h showed a significant increase in the expression of HSP70 (P = 0.0014) and pretreatment with 10 μM EA lowered the expression of HSP70 to normal levels (P = 0.0052; Figure 3E). A high expression of HSP70 after RT treatment is an early indication that RT treatment commits the cell to the apoptotic pathway.[39] However, our data indicate that a 10 μM EA pretreatment was able to reduce HSP70 expressed as a result of ER stress. These results suggest a rescue from the apoptotic pathway (Figure 3).

Mitigation of RT-Induced S-Nitrosylation of PDI and Ubiquitination. It has previously been reported that nitrosative stress can compromise the catalytic function of the oxidoreductase chaperone PDI. Specifically, the catalytic cysteines of PDI were found to be S-nitrosylated upon RT insult.[7−11] Such a chemical modification of the housekeeping machinery was found to be RT dependent and most importantly, neurotoxic.[18−21]

We examined the role of EA on mitigating levels of RT-induced S-nitroso PDI (SNO-PDI) formation. Immunoglobulin G was used to preclean the cell lysate and pulled down using

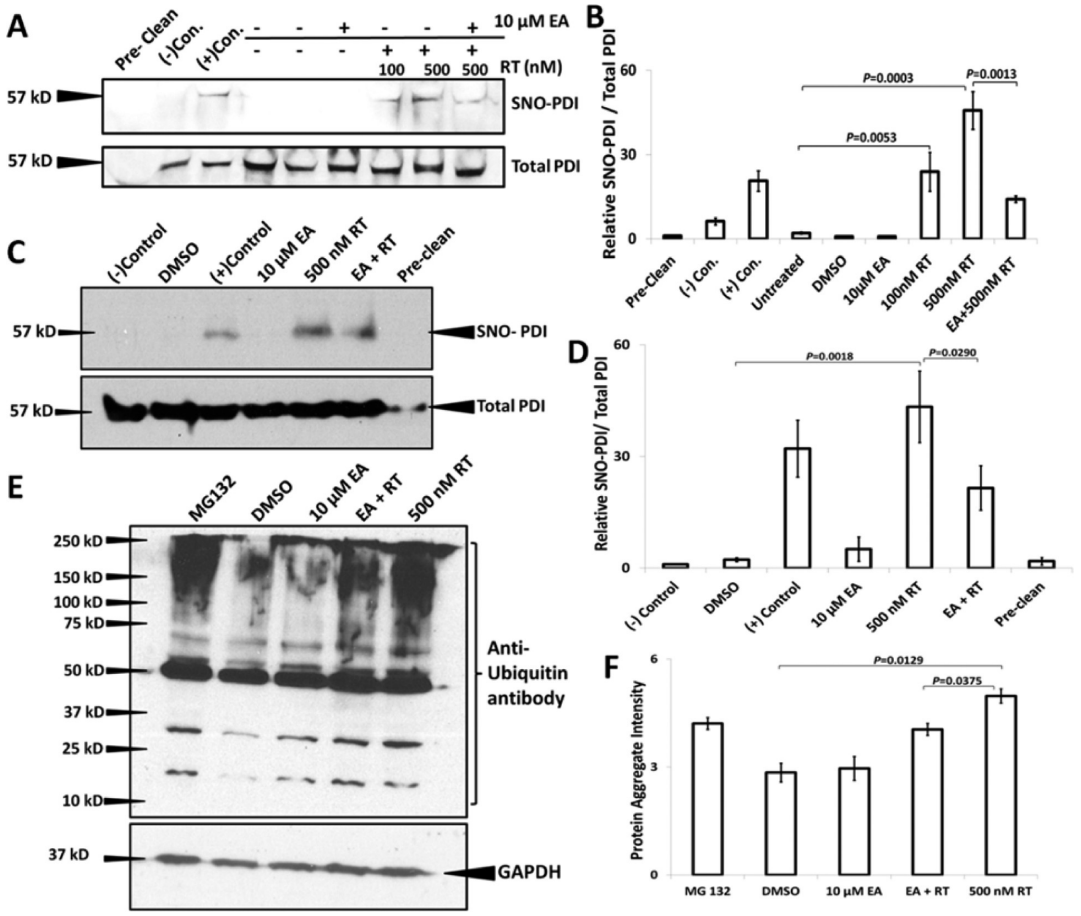

Figure 4. Evaluation of SNO-PDI formation and accumulation of ubiquitinated proteins upon different treatment. Ellagic acid (EA) successfully mitigate the rotenone (RT) induced SNO-PDI formation (A–D). SNO-PDI signals were detected after pull down the IgG-agarose beads using SNO-CYS BSA antibody then treated with PDI antibody to visualize (A). TMT-switch assay confirm the formation of SNO-PDI after RT treatment and the potential of EA (C). Densitometry analysis of SNO-PDI band (B, D). RT-induced accumulation of ubiquitinated proteins in the insoluble fraction of cell lysate is reduced after 10 μM EA pretreatment (E, F). All the densitometry analyses were done using ImageJ software from three independent tests indicated as mean ± SD. Statistical significance among pairs of samples is annotated as *P*-value (n = 3).

SNO-cysteine BSA or TMT antibody and then detected with anti-PDI antibody in this study (Pre-clean; Figure 4A, C). Dithiothreitol (DTT; negative control) S-nitrosoglutathione (positive control) treated PC12 cells were used to authenticate the experiment (Figure 4A, C). Untreated, DMSO, and 10 μM EA treated cell lysates show no formation of SNO-PDI while total PDI was expressed and identified using an anti-PDI antibody (Figure 4A, B). It is evident that pretreatment with 10 μM EA for 6 h was successfully capable of mitigating the S-nitrosylation of PDI after 500 nM RT exposure for 24 h (Figure 4A, B). The ratio of SNO-PDI versus total PDI was calculated and plotted in the bar graph to depict the true expression level of SNO-PDI upon different treatment conditions (Figure 4B, D). The different RT treatments showed a dose-dependent response when treated with 100 and 500 nM RT. The two different RT conditions showed a statistically significant difference (P = 0.0053 and 0.0003, respectively) in the formation of SNO-PDI when compared to untreated PC12 cells (Figure 4B). Pretreatment with EA showed a significant reduction (P = 0.0013) in RT induced SNO-PDI formation in PC12 cells (Figure 4B). TMT-switch assay also confirmed the SNO-PDI formation upon RT exposure (P = 0.0018) and mitigation of same when pretreated with EA (P = 0.029; Figure 4D). These results suggest that ellagic acid is able to intervene in events leading to SNO-PDI formation within the cell line. We reiterate that the actual mechanism by which EA mitigates SNO-PDI formation is not apparent from the data gathered. It may be an outcome of NO interception via peroxynitrite formation. Nevertheless, these data are consistent with previous cell-based and cell-independent in vitro results (Figures 1 and 2) indicating radical scavenging ability by the polyphenol.

Earlier studies confirmed the RT induced ER stress which is marked by overexpression of HSP70, an ER-resident protein.[39] In this study, we also showed that post-translational modification of the catalytic domain of PDI upon RT treatment for 24 h leads to ER stress and eventually activates the apoptotic pathway (Figures 2–4). PDI, an ER resident chaperone, plays a major role in proper folding of proteins.[40] Misfolded proteins are tagged by ubiquitin to guide them to proteosomal degradation system as a part of cellular defensive mechanism.[41] Overburden of the proteosomal degradation system results in accumulation of ubiquitinated proteins accompanied by an increase in protein aggregation.[41] Using antiubiquitin antibody, we demonstrated a marked increase of ubiquitinated protein after 24 h RT treatment in insoluble fractions (P = 0.0129; Figure 4E, F). However, prior treatment with EA dramatically decreased the accumulation of ubiquitinated proteins (P = 0.0375). Taken together, these data indicate that PDI plays a major role in maintaining ER

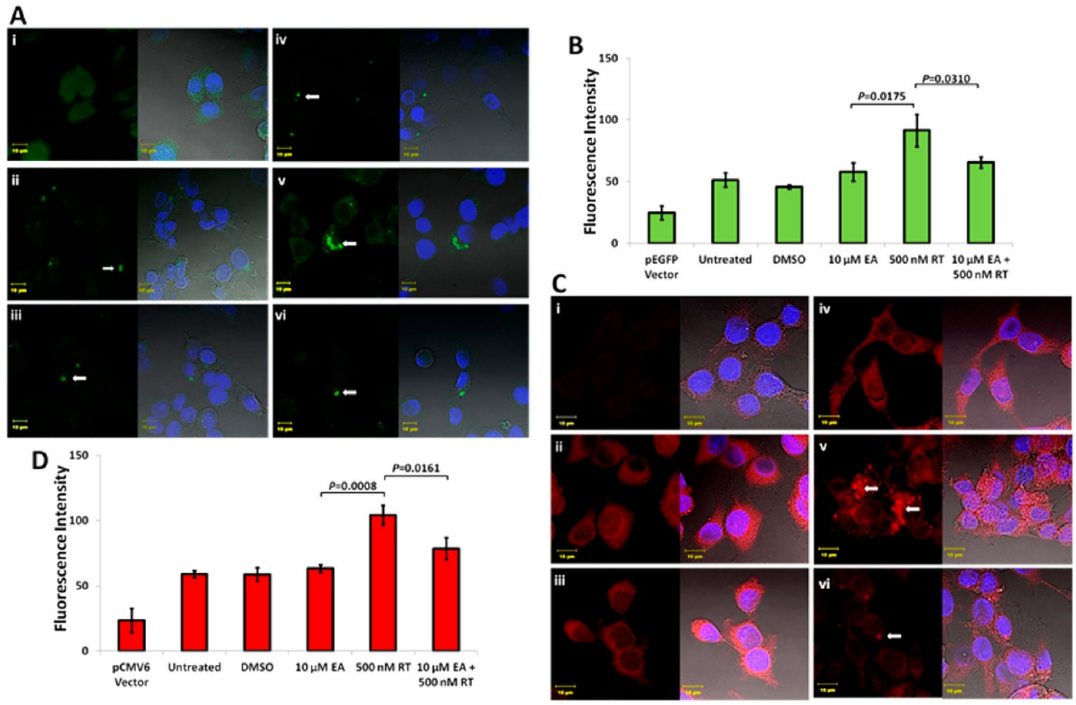

Figure 5. Role of ellagic acid (EA) in GFP-tagged synphilin-1 and α-synuclein aggregation (A–D). Cells transfected with pEGFP-C2 empty vector or pCMV6 empty vector (panel i), untreated cells (panel ii), cells treated with DMSO 2.5 v/v (panel iii), cells treated with 10 μM EA (panel iv), cells exposed to rotenone (RT) (500 nM) for 24 h alone (panel v), and cells treated with 10 μM EA for 6 h before exposed to rotenone (500 nM) for 24 h (panel vi) are the different conditions used for this study (A, C). Confocal microscopy images of PC12 cells reveal the presence of cytoplasmic aggregates in cells transfected with pEGFP-tagged synphilin-1 plasmid under different treatment (A). Confocal fluorescence images of PC12 cells revealed the presence of α-synuclein cytoplasmic aggregates under different conditions (C). All the cells were counterstained with DAPI to stain the nucleus (blue color). White arrow indicates expression of synphilin-1/α-synuclein protein (A, C). Quantification of synphilin-1 (green channel) or α-synuclein (red channel) in PC12 cell line upon different treatment using ImageJ software from n = 200 cells indicated as mean ± SD (B, D). Statistical significance between pairs of samples is illustrated as P-value. Each scale bar represents 10 μm. Each experiment was assessed in triplicate.

homeostasis and EA, a polyphenolic phytochemical, can help to prevent ER stress.

Defining the Role of EA in Synphilin-1 and α-Synuclein Aggregation. SNO-PDI formation leads to aggregation of the minor Parkinsonian biomarker synphilin-1.[10] Therefore, we examined whether prevention of SNO-PDI formation by ellagic acid intervention can mitigate the aggregation of synphilin-1. Transfected cells displayed high levels of GFP tagged syphilin-1 expression (Supporting Information Figure 2), with tendencies to be located in the cytosolic and sometimes peri-nuclear position under different treatment conditions except the empty pEGFP vector transfected cells (Figure 5A). Panel (i) indicates a relatively homogeneous cytosolic distribution of EGFP in cells transfected with pEGFP-C2 plasmid alone. In contrast, cells transfected with pEGFP–synphilin-1 constructs show a punctuated (or speckled) cytosolic distribution of green fluorescent signal (panel ii). Cells, treated with 10 μM EA alone (panel iv) did not differ in the expression of EGFP–synphilin-1 as compared to vehicle treatment (DMSO; panel iii). When cells were exposed to 500 nM rotenone for 24 h, cytosolic aggregation of synphilin-1 was clearly evident (panel v). Pretreatment of cells with 10 μM EA 6 h prior to 500 nM rotenone exposure resulted in a markedly diminished level of synphilin-1 aggregation (panel vi). These findings reveal that cells under rotenone induced nitrosative stress apparently increased the aggregation of EGFP–synphilin-1 fused protein by forming cytosolic inclusion bodies. EA showed to be able to mitigate the aggregation of the fused EGFP–synphilin-1 protein to a statistically significant level (P = 0.0310) when PC12 cells were treated with 10 μM EA prior to rotenone insult (Figure 5B).

α-Synuclein is a major Parkinsonian biomarker and the primary constituent within Lewy neurites.[14−17] We examined the expression level of α-synuclein upon rotenone toxicity (Figure 5C). Panel (ii) shows cytosolic homogeneous distribution of expressed α-synuclein when transiently transfected with pCMV6 plasmid containing α-synuclein genetic sequence. In contrast, empty pCMV6 plasmid transfection (panel i) showed no expression of α-synuclein relative to panel (ii). Disruption of the homogeneous distribution of expressed α-synuclein protein, an evident of cytosolic aggregation, was clearly seen when transiently α-synuclein transfected cells were exposed to 500 nM rotenone for 24 h (panel v). DMSO (0.1% v/v) and 10 μM EA treatment (panels ii and iv, respectively) for 24 h showed no deviation in expression level or distribution when compared with the untreated condition (panel ii). α-Synuclein transfected PC12 cells pretreated with 10 μM EA for 6 h prior to 24 h rotenone exposure are shown in panel vi. Treatment with 10 μM EA markedly reduced (P = 0.0161) the aggregated α-synuclein expression (~15% relative to RT treatment), indicating its potency to nullify the nitrosative stress imposed by rotenone exposure (Figure 5D).

EA Mitigates the Formation of RT-Induced α-Synuclein:Synphilin-1 Lewy-Body-like Inclusions. The Parkinsonian biomarkers α-synuclein and synphilin-1 are

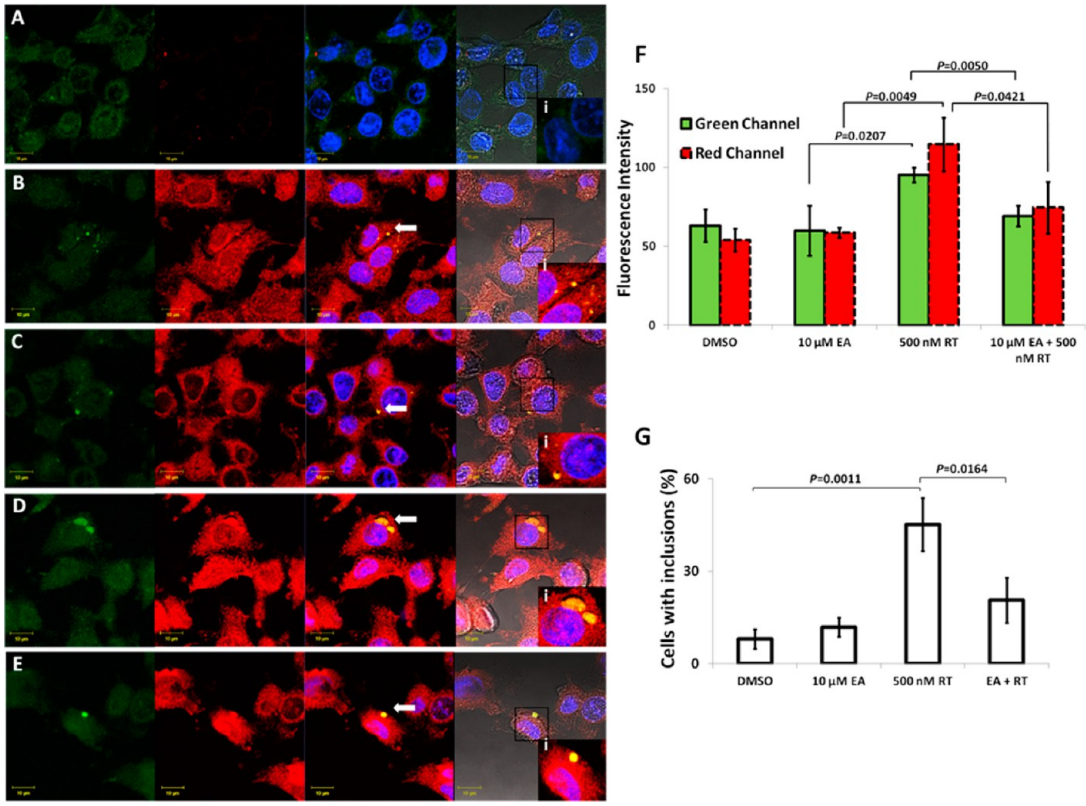

Figure 6. Coexpression of α-synuclein and synphilin-1 in PC12 cells under rotenone (RT)-induced aggregation and mitigation through ellagic acid (EA) intervention. Cells transfected with pCMV-6 and pEGFP empty vector (A). PC12 cells transfected with α-synuclein and synphilin-1 (2 μg each per condition) and treated with DMSO 0.02% v/v (B). PC12 cells were treated with 10 μM EA for 24 h (C). Cells exposed to 500 nM RT for 24 h (D). Cells pretreated with 10 μM EA for 6 h, then exposed to 500 nM rotenone for 24 h (E). Synphilin-1 was tagged with GFP showing green color, and α-synuclein is shown in red color. White arrow indicates colocalization of α-synuclein and synphilin-1 (yellow color; representative of Lewy-body-like inclusion; A–E). Inset (i) of each figure at extreme right panel zoomed in the colocalization of α-synuclein and synphilin-1 (1.5× magnification). DAPI was used to stain the nucleus (blue). Quantification of α-synuclein expression (red channel) and synphilin-1 (green channel) in PC12 cell line upon different treatment using ImageJ software from n = 200 cells indicated as mean ± SD (F). Statistical significance compared with untreated are illustrated as P-value. Each scale bar represents 10 μm. Each experiment was assessed in triplicate. Total number of cytoplasmic inclusion bodies was significantly elevated after RT treatment, although EA pretreatment decrease the inclusion body count in PC12 cells (G; Supporting Information Figure 4).

found to colocalize in PD patients' brains.[14−17] In order to investigate whether rotenone toxicity implies α-synuclein and synphilin-1 aggregation, PC12 cells were transfected with plasmid constructs carrying tagged fluorescence proteins and monitored via confocal microscopy (Figure 6). Synphilin-1 gene was fused with GFP sequence (green signal) in pEGFP plasmid, whereas α-synuclein gene (red signal as secondary antibody was conjugated with texas red probe) was inserted in pCMV6 plasmid. Colocalization of α-synuclein and synphilin-1 was detected in cells treated with 500 nM RT as evidenced by the presence of the yellow punctuated pattern (Figure 6D). The yellow pattern is the result of the superimposition of the green and red signal. The colocalization of these two biomarkers is an accepted Lewy body.[14−17] The aggregate pattern as well as colocalization were diminished when transfected PC12 cells were pretreated with 10 μM EA for 6 h prior to 500 nM RT treatment for 24 h (Figure 6E). The formation of Lewy-body-like aggregates visualized as inclusions is indicated by a white arrow in each figure except Figure 6A (cells were transfected with empty pEGFP and empty pCMV6 vector in a 1:1 ratio). A Lewy-body-like inclusion is shown as an inset (i) in the right most section of each panel zoom-in (3×) (Figure 6). Around a 2-fold increase in aggregation of synphilin-1 and α-synuclein (when coexpressed) (P = 0.0207 P = 0.0049, respectively) is clearly shown upon 500 nM RT exposure relative to the 10 μM EA treatment prior to RT exposure (Figure 6F). Results graphed as bar diagram indicate fluorescent intensity where red bar represents α-synuclein expression (red channel) and green bar represents synphilin-1 expression (green channel; Figure 6F). In the representative bar diagram, the X-axis depicts different treatment conditions and Y-axis represents fluorescent intensity (Figure 6F). Aggregation of coexpressed synphilin-1 and α-synuclein (P = 0.0050 and P = 0.0421, respectively) after rotenone exposure for 24 h in PC12 cell line was convincingly reduced by pretreatment with 10 μM ellagic acid. Colocalization of these two proteins was confirmed by using Zen 2009 software (Supporting Information Figure 3). We further counted the cytoplasmic inclusion bodies in PC12 cell cotransfected with synphilin-1 and α-synuclein (Figure 6G; Supporting Information Figure 4). The 500 nM RT treatment increased the number of inclusions dramatically relative to the vehicle control (DMSO) treatment (P = 0.0011; Figure 6G). However, cells treated with 10 μM EA prior to RT exposure had a significantly lower count of inclusion bodies (P = 0.0164). This series of experiments indicate that EA possesses protective activity against rotenone toxicity by preventing the aggregation of synphilin-1 and α-synuclein or α-synuclein:synphilin-1 Lewy-body-like inclusions in PC12 cells (Figure 6).

dx.doi.org/10.1021/cn500214k | ACS Chem. Neurosci. 2014, 5, 1209−1220

EA Binding to Human Serum Albumin (HSA). HSA is a cargo protein for different biologically active small molecules.[42] Reversible binding of a small molecule into the hydrophobic pocket of HSA can provide long shelf life as well as can help the active molecule to release into the gut for absorption.[42] In HSA, the fluorescence intensity due to the tryptophan residue (Trp-214) is proportional to the protein concentration ([P]). At the same time, this fluorescence is proportionally affected by the binding of other molecules ([L]) such as EA, thus providing a method to determine protein−ligand complex concentration ([PL]) as well as [P] and [L], ultimately providing a technique to determine binding constants.[43−45] The Langmuir isotherm data indicates that EA reversibly binds to HSA (Figure 7). The

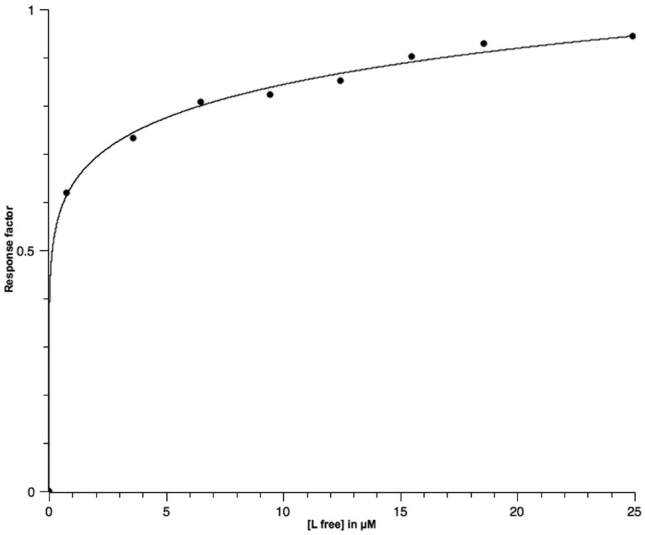

Figure 7. Fluorescence emission profiles for the binding of ellagic acid (0−140 μM) to native human serum albumin (20 μM). (A) Solid line represents a theoretical one-site binding profile. Fluorescence parameters were λ_{exc} = 280 nm and λ_{em} = 310 and 340 nm. All solutions were at 200 mM Tris-HCl, 1 mM EDTA, pH 7.5 and were prepared at room temperature 24 ± 1 °C.

K_d value for the binding of EA to HSA was experimentally determined to be $K_d = 1.43 \times 10^{-7}$ M. This reversible binding to HSA suggests that EA has an increased probability of an effective bioavailability in the human body.

CONCLUSIONS

The cytotoxicity of EA and its prophylactic effects against RT-induced nitrosative insult were determined through differential nuclear staining cytotoxicity assay. EA was found to have a low cytotoxic effect on the model PC12 cell line and a protective effect against RT cytotoxicity. Our study demonstrated that RT-induced apoptotic death evidenced by PARP-1 cleavage and flow cytometric analysis was significantly reduced in the presence of EA. EA significantly mitigated the elevated intracellular levels of ROS and RNS induced by rotenone-inhibition of the mitochondrial respiratory chain, an important finding for PD prevention and other neurodegenerative disorders associated with intracellular ROS, RNS, and ER stress. In vitro data indicate that EA gets nitrated in the presence of NOx donors. These results translate to the cell line where the presence of EA resulted in the mitigation of RNS induced S-nitrosylation of PDI. The mechanism by which SNO-PDI formation is mitigated by EA could be through the consumption of NO generated peroxynitite.[30,32]

These data represent an important finding in the methods designed to prevent pathogenesis of sporadic PD. EA intervention was also found to play an important role mitigating the formation of α-synuclein and synphilin-1 aggregates as well as α-synuclein:synphilin-1 Lewy-body-like aggregates by maintaining ER homeostasis. In addition, EA was found to have a strong interaction with HSA, which has implications in drug bioavailability.

In conclusion, our results advance the neurodegeneration field by mapping the catalytic failure of cellular housekeeping machinery to PD and also establish a preventative approach against the disease. The reported results can be used for further research in related neuropathies whose onset may be related to the dysfunction of the cellular homeostasis apparatus. It is especially noteworthy that EA has no known side effects and crosses the blood-brain barrier.[28]

METHODS

Reagents, Cell Line, and Plasmid. Ellagic acid, rotenone (RT), 2′,7′-dichlorodihydrofluorescein diacetate (DCFH-DA), tetranitromethane (TNM), and 4-amino-5-methylamino-2″,7″-difluorofluorescein diacetate (DAF-FM DA) were purchased for the study (Sigma-Aldrich E2250, R8875, D6883, T25003 and Life Technologies D-23842, respectively). Other commercially sourced reagents were as follows: Mouse monoclonal for GAPDH antibody (glyceraldehyde 3-phosphate dehydrogenase), poly(ADP-ribose) polymerase antibody, ubiquitin antibody (Cell Signaling Technology; 3683, 46D11, 3933, respectively), protein disulfide isomerase antibody (Abcam; ab2792), HSP70 antibody (SantaCruzBio; sc-66048), Hoechst 33342 (Life Technologies; H1399), propidium iodide (PI) (MP Biomedicals, 195458), annexin V kit (Beckman Coulter; IM3546), horseradish peroxidase (HRP)-conjugated goat anti-mouse and anti-rabbit antibody (KPL Biomedical, 214-1806 and 214-1516), and rat pheochromocytoma derived neuronal PC12 cells (ATCC number: CRL-1721) from a male origin. Cells were transfected with the pEGFP-C2 or synphilin-1/pEGFP-C2 and pCMV6 or α-synuclein/pCMV6 plasmid (NCBI Reference Sequence: NM_001146054.1) as described.[46] Serum albumin from human ≥99% fatty acid free was obtained from Sigma-Aldrich (A9511). DM45 spectrofluorimeter was obtained from Olis online instruments systems, Inc. (Bogart, GA).

Mass Spectrometry Assay. Ellagic acid stock solution was prepared in acetonitrile and then diluted to obtain concentrations ranging from 0.1 to 80 μM (in acetonitrile). TNM was added from a stock solution (freshly prepared by weight in acetonitrile) to EA at different ratios. The samples were analyzed on a Q-TOF ESI negative mode mass spectrometer.

Cell Culture and Transfection. PC12 cells were cultured in Dulbecco's modified Eagle's medium (DMEM) supplemented with 10% fetal bovine serum, 100 U/mL penicillin, and 100 μg/mL streptomycin. Cells were routinely grown at 37 °C in humidified 5% carbon dioxide atmosphere in complete DMEM media. Trypsin-EDTA 0.25% (1×) (Life Technologies, 25200-056) was used to detach the cells from the culture surface when needed, and once detached complete DMEM media was added to the cell suspension. Subsequently, the cell suspension was centrifuged at 900 rpm for 5 min in order to remove trypsin from incubation media. Cell transfections were performed the following day after plating. Subsequently, cell transfections were performed with pEGFP-C2 control (without insert) or pEGFP-C2 carrying the fusion protein GFP-synphilin-1 and pCMV6 control or pCMV6 inserted with α-synuclein as recommended by manufacturer using Lipofectamine LTX with Plus reagent (Life Technologies; 15338500). Transfected cells were incubated overnight to allow expression of transfection complexes under normal growth condition for expression of pEGFP-C2/pCMV6 (control) or the complex pEGFP-C2 with synphilin1/

pCMV6 with α-synuclein gene and both at the same time at a ratio of 1:1. Transiently transfected PC12 cells were incubated overnight to allow expression of proteins.

Differential Nuclear Staining Cytotoxicity Assay. Cells were seeded into 96-well plates and incubated for 24 h to allow attachment. Subsequently, cells were treated with different concentrations of RT or EA to determine its possible cytotoxic effects. As control for nonspecific effects, DMSO vehicle control, as contained in the experimental samples, was included at final concentration of 0.5% v/v. In addition, in order to measure the ability of RA to intervene and protect against rotenone insult, cells were pretreated with 10 μM EA for 6 h prior to rotenone exposure. Subsequently, cells were incubated for an additional 24 h and images were captured in live mode. A mixture of PI and Hoechst 33342 at a final concentration of 1 μg/mL was added to each well 1 h prior to imaging.[46] Images were acquired in a live-cell mode utilizing a BD Pathway 855 Bioimager system (BD Biosciences Rockville, MD). Montages (3 × 3) from nine adjacent image fields were captured per well utilizing a 10× objective. Image capture and data analysis determining the percentage of cell death per each individual well were achieved by using BD AttoVision v1.6.2 software[46] (BD Biosciences Rockville, MD). Each experimental point was assessed in quintuplicate.

Detection of Intracellular ROS and RNS. Intracellular ROS and RNS levels were measured using the oxidation-sensitive fluorescent probes DCFH-DA and DAF-FM DA, respectively. Cells were seeded (5000/well) on a 96-well plate and treated with 10 μM DCFH-DA or 5 μM DAF-FM in 50 μL of DMEM media according to the manufacturer's protocol. After treatment, cells were analyzed with a microplate reader fluorometer (Labsystems Fluoroskan Ascent) using excitation at 485 nm and emission at 518 nm. Each data point was assessed in quintuplicate. Images were captured using a Carl Zeiss LSM 700 microscope, 20× lens.

Apoptosis/Necrosis Assay Using Fluorescence-Activated Cell Sorting. Cells were seeded on a 24-well microplate at a density of 20 000 cells/well and cultured as previously described. Cells were incubated for 6 h in the presence of EA and then treated with RT and incubated for an additional 24 h. Cells from each individual well were washed, collected, and processed essentially as previously described.[46] Briefly, cells were concurrently stained by resuspending them in a solution containing annexin V-FITC and PI dissolved in 100 μL of binding buffer. After incubation for 15 min on ice and in the dark, ice-cold binding buffer (400 μL) was added to the cell suspensions. The mixture was gently homogenized and immediately analyzed by flow cytometry. The percentage of total apoptotic cells per sample is annotated as the sum of both early and late stages of apoptosis (annexin V-FITC positive), bottom right quadrant and top right quadrant, respectively.[46] For each sample, approximately 10 000 individual events were acquired using a flow cytometer (Cytomics FC 500; Beckman Coulter) and data analyzed with CXP software (Beckman Coulter). Each data point was assessed in quintuplicate.

Western Blot Analysis. Total soluble cell lysates were prepared by washing the cells with cold Tris-buffered saline, collected by centrifugation (3003*g*, 5 min at 4 °C, and extracted by sonication in buffer containing 10 mM Tris-HCl (pH 7.4), 10 mM EDTA, 0.5% (w/v) SDS, protease and phosphatase inhibitors (Thermo Fisher Scientific; 78442). The insoluble cell pellet was boiled for 30 s after dissolving in 3× sample buffer (without βmarcaptoethanol) and centrifuged for 1 min before loading for SDS-polyacrylamide gel electrophoresis[46] (SDS-PAGE). We used the insoluble protein fraction to detect accumulation of ubiquitinated proteins. On the other hand, after quantification, equal amounts of soluble cell lysates (approximately 20 μg per lane) were separated using SDS-PAGE and then transferred to polyvinyldifluoride (PVDF) membranes. Blots were incubated in 5%, w/v, dried skim milk/Tris-buffered saline pH 7.4, and 0.1% Tween 20 (TBST) followed by incubation for 2 h with anti-PARP/anti-α-synuclein/anti-PDI/anti-HSP70/antiubiquitin monoclonal antibodies (1:1000) or anti-GAPDH (loading control; 1:1000) diluted in 3% BSA/TBST. After washes, blots were exposed to secondary antibodies by incubating for 1 h with horseradish peroxidase (HRP)-conjugated goat anti-rabbit antibody in 5% dry skim milk/TBST for 30 min. Chemiluminescence (SuperSignal West Pico Chemiluminescent Substrate; Thermo Fisher Scientific; 34077) was used according to the manufacturer's instructions. Each data point was assessed in triplicate.

Coimmunoprecipitation and Tandem Mass Tag (TMT)-Switch Assay. Cell lysates were prepared following the same procedure used for Western blot. To prepare positive and negative controls, cells were incubated for 30 min at room temperature with 200 μM *S*-nitrosoglutathione or DTT, respectively. Proteins were separated via 10% SDS-PAGE, blotted, and visualized with specific antibodies. For detection of S-nitrosylated PDI, 200 μL of lysates (1 mg/mL) of PC12 cell homogenates were precleared by the addition of 50 μL of protein G agarose[47] (Santa Cruz Biotechnology). Next, 2.5 μg of polyclonal anti-*S*-nitrosocysteine antibody (Abcam; ab50185) or normal rabbit IgG (SantaCruzBio; sc-2027) was added to the supernatant, and the mixture incubated for 1 h at 4 °C with agitation. Immunocomplexes were precipitated by the addition of 50 μL of protein G agarose, followed by incubation for 1 h at 4 °C with agitation and then centrifugation at 5000 rpm for 2 min. The pellets were then washed thrice with 1 mL of chilled TBS containing 1% (v/v) Tween-20 and 1 mg/mL BSA and once with 0.5 M Tris-HCl. Following the final centrifugation step, the pellet was resuspended in SDS sample buffer, subjected to Western blot analysis, and immunostained for PDI as described previously. We also used the Pierce S-Nitrosylation Western Blot Kit (Thermo Fisher Scientific; 90105) to detect S-nitrosylated protein modification. This assay was performed following manufacturer instructions. In short, we used anti-TMT antibody to pull down the cell lysate then detected using anti-PDI antibody. Each data point was assessed in triplicate.

Confocal Microscopy and Immunocytochemistry. Cells transfected with empty vector or with EGFP-synphilin-1/α-synuclein insert were washed after treatment, fixed with 4% paraformaldehyde in PBS, stained with DAPI, and the mounted under ProLong antifade medium (Molecular Probes). To stain for synphilin-1/α-synuclein proteins, cells were fixed as above, permeabilized with 0.1% (w/v) saponin in PBS, blocked with PBS plus 5% goat serum, 5% FBS, and 0.1% TWEEN 20, followed by incubation with primary antibody (overnight at 4 °C) and secondary rhodamine-conjugated goat anti-mouse antibody[46] (1:10000; KPL Biomedical). Fluorescence confocal images were captured utilizing a LSM 700 confocal microscope and assisted with ZEN 2009 software (Zeiss, New York, NY).

Immunoblot, Immunofluorescence, and Inclusion Body Quantification. To quantify protein expression and fluorescence intensity, we used the open source software ImageJ. Each logical storage manager (LSM) format data were opened in ImageJ and converted into RGB file (8 bit). In order to quantify the fluorescence of expressed proteins, random fields for each tested condition were obtained at the same magnification (63× oil immersion objective, zoom 1.5×). Then, a region of interest (ROI) with an area of 400 pixels (20 × 20) was chosen, and the average intensity of fluorescence within the ROI was measured in the cytosol of every transfected cell present in the field. Over 200 cells were analyzed for each condition. The values obtained were averaged and were plotted using a bar graph. The results were obtained from more than or equal to three independent experiments. Colocalization of two different fluorescently labeled proteins was determined using ZEN 2009 software[46] (Zeiss; Supporting Information Figure 3). To count the cells with inclusion bodies, we used colocalization finder in ImageJ software. Randomly selected 5 different fields with more than 200 cells/field were counted in three different sets of experiments to avoid prejudice (Supporting Information Figure 4).

Protein Binding Assay. EA from a stock solution of 2.4 mM was aliquoted in a solution of 20 μM serum albumin from human (HSA) (pH 7.5, 20 mM Tris-HCl). Fluorescence emission spectra were obtained 5 min after every titration by scanning the emission from 310 to 340 nm (Ext. 280 nm; DM45 sptecroflurimeter, Olis Instruments, GA). The quenching of fluorescence was fitted to a binding curve.[43−45]

Statistical Calculation. Every data point was collected independently and in triplicate. To note experimental viability and variability, data were presented as the average with corresponding standard

deviation. Statistical analysis was performed using two-tailed paired Student's *t* test to denote the statistical significance of variances between experimental samples and their corresponding controls. To identify if there is a significant difference between two groups, a value of $P < 0.05$ was considered significant. We denote the actual *P*-value in each graph wherever needed.

■ ASSOCIATED CONTENT

Supporting Information

Live PC12 cell imaging to determine cytotoxicity (Supplementary Figure 1), overexpression of α-synuclein in PC12 cell (Supplementary Figure 2), colocalization quantification of α-synuclein and synphilin-1-GFP (Supplementary Figure 3), quantification of inclusion bodies in PC12 cell (Supplementary Figure 4), specificity of *S*-nitrosocysteine antibody (Supplementary Figure 5), and analytical data (mass spectrometry analysis) of ellagic acid and TNM (Table S1). This material is available free of charge via the Internet at http://pubs.acs.org.

■ AUTHOR INFORMATION

Corresponding Author

*E-mail: mnarayan@utep.edu. Phone: 915-747-6614. Fax: 915-747-5748. Mailing address: 500 W. University Ave., Chemistry and Computer Science Building 2.0202, El Paso, Texas 79968, United States.

Author Contributions

P.K. conceptualized, designed and performed experiments, analyzed all the in vivo data, and wrote the manuscript. J.E.M. helped P.K. with cytotoxicity and ROS assays. In addition, J.E.M. did the binding assay, helped to analyze Figure 7 data, helped to edit the figures, and corrected the manuscript. E.Z. performed the mass spectrometry assay and analyzed Figure 1. A.V-R. provided technical help in cytotoxicity assay and flow cytometry experiments as well as edits to the figures and manuscript. M.N. conceived the project and reviewed the data and manuscript.

Funding

This study was supported funding from the Alzheimer's disease Research Foundation to M.N. J.E.M. would like to thank Campus Office of Undergraduate Research Initiatives (COURI) at UTEP for the support.

Notes

The authors declare no competing financial interest.

■ ACKNOWLEDGMENTS

The authors would like to express special thanks to the staff of the Cytometry, Screening, and Imaging Core Facility of the Border Biomedical Research Center at The University of Texas at El Paso (UTEP). This facility is supported by Grant # 2G12MD007592 and Grant # 5G12MD007592 from the Research Centers in Minority Institutions program of the National Institutes on Minority Health and Health Disparities. In addition, M.N. would like to thank the College of Science (Research Enhancement Award) at UTEP and Dr. Eddie Vazquez and Mrs. Holly Vazquez (The El Paso Pain Center) for their financial support.

■ ABBREVIATIONS

PD, Parkinson's disease; AD, Alzheimer's disease; PC12, pheochromocytoma cell; EA, ellagic acid; RT, rotenone; GFP, green fluorescent protein; PDI, protein disulfide isomerase; LBVAD, Lewy body variant of Alzheimer's Disease; ROS, reactive oxygen species; PARP, poly(ADP-ribose) polymerase; HSP70, heat shock protein 70; HSA, human serum albumin; TNM, tetranitromethane; SNO, S-nitrosylated

■ REFERENCES

(1) Findley, L. J. (2007) The economic impact of Parkinson's disease. *Parkinsonism & Relat. Disord. 13* (Supplement), S8−S12.
(2) Meek, P. D., McKeithan, E. K., and Schumock, G. T. (1998) Economic Considerations in Alzheimer's Disease. *Pharmacotherapy 18*, 68−73.
(3) Moretto, A., and Colosio, C. (2013) The role of pesticide exposure in the genesis of Parkinson's disease: Epidemiological studies and experimental data. *Toxicology 307*, 24−34.
(4) Pezzoli, G., and Cereda, E. (2013) Exposure to pesticides or solvents and risk of Parkinson disease. *Neurology 80*, 2035−2041.
(5) Gilbert, H. F. (1998) Protein disulfide isomerase. *Methods Enzymol. 290*, 26−50.
(6) Narayan, M. (2012) Disulfide bonds: protein folding and subcellular protein trafficking. *FEBS J. 279*, 2272−2282.
(7) Benham, A. M. (2012) The Protein Disulfide Isomerase (PDI) family: key players in health and disease. *Antioxid. Redox Signaling 16*, 781−789.
(8) Benhar, M., Forrester, M. T., and Stamler, J. S. (2006) Nitrosative stress in the ER: a new role for S-nitrosylation in neurodegenerative diseases. *ACS Chem. Biol. 1* (6), 355−358.
(9) Nakamura, T., and Lipton, S. A. (2011) S-nitrosylation of critical protein thiols mediates protein misfolding and mitochondrial dysfunction in neurodegenerative diseases. *Antioxid. Redox Signaling 14*, 1479−1492.
(10) Uehara, T., Nakamura, T., Yao, D., Shi, Z. Q., Gu, Z., Ma, Y., Masliah, E., Nomura, Y., and Lipton, S. A. (2006) S-nitrosylated protein-disulphide isomerase links protein misfolding to neurodegeneration. *Nature 441*, 513−517.
(11) Uehara, T. (2007) Accumulation of misfolded protein through nitrosative stress linked to neurodegenerative disorders. *Antioxid. Redox Signaling 9*, 597−601.
(12) Kieburtz, K. (2010) Discovering neuroprotection in Parkinson's disease, or getting to haphazard. *Mt. Sinai J. Med. 77*, 700−6.
(13) Narayan, M. (2011) Factors impacting fold maturation of ER-processed proteins: The case of oxidative folding of ribonuclease A. In *Folding of disulfide proteins* (Chang, R. J. Y., Ventura, S., Eds.), Protein Reviews (Atassi, M. Z., Series Ed.), Vol. *14*, pp 23−42, Springer, New York.
(14) Baba, M., Nakajo, S., Tu, P. H., Tomita, T., Nakaya, K., Lee, V. M., Trojanowski, J. Q., and Iwatsubo, T. (1998) Aggregation of alpha-synuclein in lewy bodies of sporadic Parkinson's disease and dementia with Lewy bodies. *Am. J. Pathol. 152*, 879−884.
(15) Kawamata, H., McLean, P. J., Sharma, N., and Hyman, B. T. (2001) Interaction of alpha-synuclein and synphilin-1: effect of Parkinson's disease-associated mutations. *J. Neurochem. 77*, 929−934.
(16) Neystat, M., Rzhetskaya, M., Kholodilov, N., and Burke, R. E. (2002) Analysis of synphilin-1 and synuclein interactions by yeast two-hybrid beta-galactosidase liquid assay. *Neurosci. Lett. 325*, 119−123.
(17) Spillantini, M. G., Schmidt, M. L., Lee, V. M., Trojanowski, J. Q., Jakes, R., and Goedert, M. (1997) Alpha-synuclein in Lewy bodies. *Nature 388*, 839−840.
(18) Hess, D. T., Matsumoto, A., Kim, S.-O., Marshall, H. E., and Stamler, J. S. (2005) Protein S-nitrosylation: purview and parameters. *Nat. Rev. Mol. Cell Biol. 6*, 150−166.
(19) Mattson, M. P. (2006) Nitro-PDI incites toxic waste accumulation. *Nat. Neurosci. 9*, 865−867.
(20) Walker, A. K., and Atkin, J. D. (2011) Mechanisms of neuroprotection by protein disulphide isomerase in amyotrophic lateral sclerosis. *Neurology Res. Int. 2011*, 317340 DOI: 10.1155/2011/317340.
(21) Walker, A. K., Farg, M. A., Bye, C. R., McLean, C. A., Horne, M. K., and Atkin, J. D. (2010) Protein disulphide isomerase protects

against protein aggregation and is S-nitrosylated in amyotrophic lateral sclerosis. *Brain 133*, 105−116.
(22) Haldar, S. M., and Stamler, J. S. (2011) S-Nitrosylation at the interface of autophagy and disease. *Mol. Cell 43*, 1−3.
(23) Uys, J. D., Xiong, Y., and Townsend, D. M. (2011) Nitrosative stress-induced S-glutathionylation of protein disulfide isomerase. *Methods Enzymol. 490*, 321−332.
(24) Osawa, T., Ide, A., Su, J. D., and Namiki, M. (1987) Inhibition of lipid peroxidation by ellagic acid. *J. Agric. Food Chem. 35*, 808−812.
(25) Thresiamma, K. C., and Kuttan, R. (1996) Inhibition of liver fibrosis by ellagic acid. *Indian J. Physiol. Pharmacol. 40*, 363−366.
(26) Abou-Zied, O., and Al-Shihi, O. (2008) Characterization of Subdomain IIA Binding Site of Human Serum Albumin in its Native, Unfolded, and Refolded States Using Small Molecular Probes. *J. Am. Chem. Soc. 130*, 10793−10801.
(27) Dockal, M., Carter, D. C., and Rüker, F. (1999) The Three Recombinant Domains of Human Serum Albumin: Structural Characterization and Ligand Binding Properties. *J. Biol. Chem. 274*, 29303−29310.
(28) Borges, G., Roowi, S., Rouanet, J.-M., Duthie, G. G., Lean, M. E. J., and Crozier, A. (2007) The bioavailability of raspberry anthocyanins and ellagitannins in rats. *Mol. Nutr. Food Res. 51*, 714−725.
(29) Pacher, P., Beckman, J. S., and Liaudet, L. (2007) Nitric oxide and peroxynitrite in health and disease. *Physiol. Rev. 87*, 315−424.
(30) Cimino, F., Anderson, W. B., and Stadtman, E. R. (1970) Ability of Nonenzymic Nitration or Acetylation of E. coli Glutamine Synthetase to Produce Effects Analogous to Enzymic Adenylylation. *Proc. Natl. Acad. Sci. U. S. A. 66*, 564−571.
(31) Radi, R., Beckman, J. S., Bush, K. M., and Freeman, B. A. (1991) Peroxynitrite oxidation of sulfhydryls. The cytotoxic potential of superoxide and nitric oxide. *J. Biol. Chem. 266*, 4244−4250.
(32) Barbara, S. B., Rodney, L. L., and Earl, R. S. (1998) Carbon dioxide stimulates peroxynitrite-mediated nitration of tyrosine residues and inhibits oxidation of methionine residues of glutamine synthetase: Both modifications mimic effects of adenylylation. *Proc. Natl. Acad. Sci. U. S. A. 95*, 62784−2789.
(33) Aranda, A., Sequedo, L., Tolosa, L., Quintas, G., Burello, E., Castell, J. V., and Gombau, L. (2013) Dichloro-dihydro-fluorescein diacetate (DCFH-DA) assay: A quantitative method for oxidative stress assessment of nanoparticle-treated cells. *Toxicol. In Vitro 27* (2), 954−963.
(34) Eruslanov, E., and Kusmartsev, S. (2010) Identification of ROS Using Oxidized DCFDA and Flow-Cytometry. *Methods Mol. Biol. 594*, 57−72.
(35) Kojima, H., Urano, Y., Kilkuchi, K., Higuchi, K., Hirata, Y., and Nagano, T. (1999) Fluorescent Indicators for Imaging Nitric Oxide Production. *Angew. Chem., Int. Ed. Engl. 38* (21), 3209−3212.
(36) Tanner, C. M., Kamel, F., Ross, G. W., Hoppin, J. A., Goldman, S. M., Korell, M., Marras, C., Bhudhikanok, G. S., Kasten, M., Chade, A. R., Comyns, K., Richards, M. B., Meng, C., Priestley, B., Fernandez, H. H., Cambi, F., Umbach, D. M., Blair, A., Sandler, D. P., and Langston, J. W. (2011) Rotenone, paraquat, and Parkinson's disease. *Environ. Health Perspect. 119* (6), 866−872.
(37) Burkart, V., Wang, Z.-Q., Radons, J., Heller, B., Herceg, Z., Stingl, L., Wagner, E. F., and Kolb, H. (1999) Mice lacking the poly(ADP-ribose) polymerase gene are resistant to pancreatic beta-cell destruction and diabetes development induced by streptozocin. *Nat. Med. 5*, 314−319.
(38) Oliver, F. J., de la Rubia, G., Rolli, V., Ruiz-Ruiz, M. C., Murcia, G., and Murcia, J. M. (1998) Importance of poly(ADP-ribose) polymerase and its cleavage in apoptosis. Lesson from an uncleavable mutant. *J. Biol. Chem. 273*, 33533−33539.
(39) Ryu, E. J., Harding, H. P., Angelastro, J. M., Vitolo, O. V., Ron, D., and Greene, L. A. (2002) Endoplasmic Reticulum Stress and the Unfolded Protein Response in Cellular Models of Parkinson's Disease. *J. Neurosci. 22* (24), 10690−10698.
(40) Gruber, C. W., Čemažar, M., Heras, B., Martin, J. L., and Craik, D. J. (2006) Protein disulfide isomerase: the structure of oxidative folding. *Trends Biochem. Sci. 31* (8), 455−464.
(41) Glickman, M. H., and Ciechanover, A. (2002) The ubiquitin-proteasome proteolytic pathway: destruction for the sake of construction. *Physiol. Rev. 82* (2), 373−428.
(42) Adams, P. A., and Berman, M. C. (1980) Kinetics and mechanism of the interaction between human serum albumin and monomeric haemin. *Biochem. J. 192* (1), 95−102.
(43) Lakowicz, J. R. (1999) *Principles of Fluorescence Spectroscopy*, 2nd ed., Kluwer/Plenum, New York.
(44) Mandeville, J., Froehlich, E., and Tajmir-Riahi, H. A. (2009) Study of curcumin and genistein interactions with human serum albumin. *J. Pharm. Biomed. Anal. 49*, 468−474.
(45) N'soukpoé-Kossi, C. N., Sedaghat-Herati, R., Ragi, C., Hotchandani, S., and Tajmir-Riahi, H. A. (2007) Retinol and retinoic acid bind human serum albumin: Stability and structural features. *Int. J. Biol. Macromol. 40*, 484−490.
(46) Kabiraj, P., Pal, R., Varela-Ramirez, A., Miranda, M., and Narayan, M. (2012) Nitrosative stress mediated misfolded protein aggregation mitigated by Na-D-β-hydroxybutyrate intervention. *Biochem. Biophys. Res. Commun. 426* (3), 438−444.
(47) Wu, M., Katta, A., Gadde, M. K., Liu, H., Kakarla, S. K., Fannin, J., Paturi, S., Arvapalli, R. K., Rice, K. M., Wang, Y., and Blough, E. R. (2009) Aging-associated dysfunction of Akt/protein kinase B: S-nitrosylation and acetaminophen intervention. *PLoS One 4* (7), e6430.